



Magnetic fabrics and petrofabrics: their orientation distributions and anisotropies

Graham J. Borradaile*

Geology Department, Lakehead University, Thunder Bay, Canada P7B 5E1

Received 14 September 2000; revised 25 January 2001; accepted 30 January 2001

Abstract

Magnetic-fabric and other petrofabric anisotropies may be described by second-rank tensors represented by ellipsoids. For a homogeneous petrofabric that is adequately sampled, a stereoplot of the orientation-distribution of the tensors' principal axes (maximum, intermediate and minimum) should show three orthogonal concentrations. The concentrations form some combination of shapes from circular clusters through partial girdles to full girdles. The concentrations' elliptical eccentricities are constrained by the symmetry of the sample-orientation-distribution (i.e. L , $L > S$, $L = S$ etc.) as well as the individual sample-anisotropies. The mean orientations of principal axes must be orthogonal, just as with individual sample-tensors. This requires tensor-statistics for their calculation (Jelinek, 1978). Furthermore, elliptical confidence cones for the means should parallel principal planes, preserving overall orthorhombic symmetry. However, in practice, sub-orthorhombic symmetry may arise from unrepresentative sampling but it may also be a useful indicator of multiple or heterogeneous petrofabrics. In the case of magnetic fabrics, the wide range in average susceptibility values and variation in magnetic mineralogy permit small numbers of high-susceptibility samples to deflect the orientation of the tensor-mean away from the majority of samples. Normalizing the samples by their bulk susceptibility overcomes this, but the orientation of high-susceptibility outliers may signify an event or subfabric of importance that we should not discard. Therefore, stereoplots of both normalized and non-normalized orientation-distributions should be compared, preferably also identifying the outliers. It is important to distinguish the shape of the orientation distribution ellipsoid from the shape of the individual magnetic fabric ellipsoids. (The qualitative L–S nomenclature is best replaced by T_j where $T_j = +1 =$ oblate; $T_j = -1 =$ prolate (Jelinek, 1981).) Invariably, the orientation distribution is described by an ellipsoid whose shape is more spherical than that of the individual sample-anisotropy ellipsoids because the latter have scattered orientations. Furthermore, the shape of the orientation-distribution ellipsoid need bear no relation to the shape of individual sample-ellipsoid anisotropies. The concepts are illustrated with 1119 measurements of anisotropy of magnetic susceptibility (AMS) from seven areas and with 188 measurements of anisotropy of anhysteretic remanence (AARM) from two areas. © 2001 Elsevier Science Ltd. All rights reserved.

Keywords: Magnetic fabric; Petrofabric; Tensor statistics; Orientation-distribution symmetry; Orthorhombic fabric symmetry

1. Introduction

The distribution of orientations in three-dimensions interests several fields of earth science, especially structural geology, petrofabrics and paleomagnetism. In particular, the characterization of a mean orientation and the dispersion about it require some attention, even where the data form a unimodal cluster with circular symmetry. Two clear lines of analysis follow. First, one may deal with axes (non-directed lines) such as fold axes, mineral lineations, petrofabric alignments and magnetic susceptibility axes that may be represented on one hemisphere of a stereogram. Most orientation data in structural geology fall into this category, with the notable exceptions of younging directions of strata,

facing directions of folds, vergence directions of tectonic movements and paleocurrent directions. These, like paleomagnetic directions and geomagnetic flux possess a polarity requiring both upper and lower hemispheres for their projection. Fisher et al. (1987) reviewed most aspects of this subject and describe the different statistical treatments required to determine the mean orientations, variances and perform hypothesis tests for sample-distributions, where an appropriate theoretical model may be assumed.

Before we proceed further, we must establish the concept of a homogeneous petrofabric. If the orientation distribution of the property that we consider is the same throughout a sample, it can be said to possess a homogeneous petrofabric. If the property was identically oriented throughout, then the petrofabric would have a saturation alignment and there would be no dispersion of the directions and the mean direction would be defined automatically. The latter situation

* Tel.: +1-807-343-8461; fax: +1-807-935-2753.

E-mail address: borradaile@lakeheadu.ca (G.J. Borradaile).

may be approached where stress-induced nucleation of metamorphic minerals produces a very strong alignment. More generally, the petrofabric is represented by an imperfect alignment but is nevertheless homogeneous, at least at the sample scale. The general problem is, given a suite of such samples from different locations, how do we characterize the petrofabric variation? Whether the different locations are from a single site or outcrop, or from several sites spread over an area, any straightforward statistical treatments require a higher level of fabric homogeneity. The dispersion of directions from one outcrop to another must define an inter-site orientation distribution that is also homogenous. As a shorthand description of such directional variation, Flinn (1965) introduced the concept of a fabric ellipsoid, varying continuously in shape from oblate, for a dispersion of axes in a plane (e.g. schistosity, foliation = S) to prolate for a dispersion of axes about one direction (e.g. a linear fabric = L). Structural geologists use Flinn's L–S scheme in connection with dimensions of aligned (perhaps strained) objects so that these are sometimes referred to as flattened (S) and constricted (L) fabrics, with the gamut of possibilities between (Fig. 1).

The determination of the mean direction and calculation of dispersion generally involves the assumption of some mathematical model for the spherical frequency distribution (Fisher et al., 1987, p. 67 et seq.). Different treatments are

required for vectors and axes and they must take account of anisotropic clusters, partial and full girdles to be of value in structural geology, petrofabrics or paleomagnetism. Fisher et al. (1987, p. 84 et seq.) recommend the Kent distribution for vectors and the Watson distribution for axes. Natural orientation distributions are imperfect representations of girdles or clusters, with ragged contours and sub-clusters. These may be artefacts of sampling and limited sample-size, in which case statistics calculated using one of the theoretical models may be appropriate: the low confidence of the resulting mean direction is a meaningful measure of uncertainty. Alternatively, it is common for two geological processes to be compounded so that two petrofabric orientation-distributions are inappropriately merged: the resulting statistics may then be meaningless. Unfortunately, it may not be simple to discriminate between these possibilities from geological data and it is usually impossible from the orientation distribution alone.

The initial and most objective characterization of any orientation distribution is to produce some sort of density plot, familiar to structural geologists as contoured stereograms. Visual inspection alerts one to the possibilities of inter-site heterogeneity, subarea-homogeneity and the validity of any statistics that are calculated. Subsequently, it may be possible to associate the separate, more homogeneous sub-populations with different subareas. In this

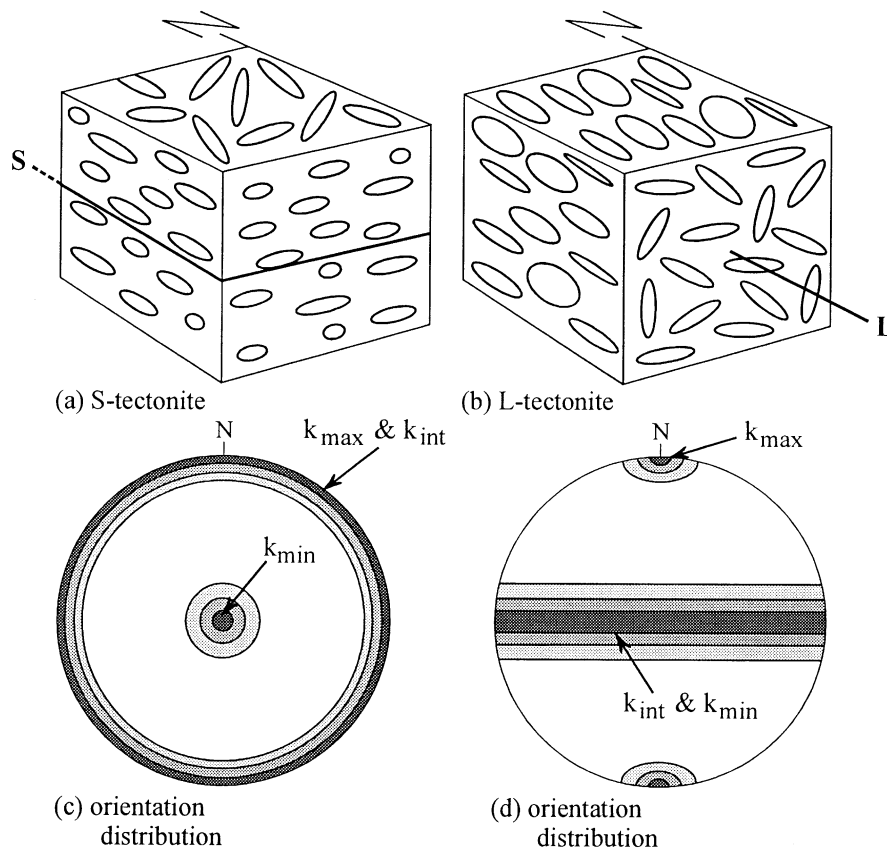


Fig. 1. (a, b) S- and L-tectonite terminology for orientation distributions of objects (in this case, AMS sample-ellipsoids) (Flinn, 1965). (c, d) associated stereograms showing contours of principal susceptibility axes for ideal L- and S-tectonites.

simple scenario, a homogeneous petrofabric simply shows *spatial variation* on a regional scale. Alternatively, and more commonly than is sometimes realized, different subpopulations of the orientation distribution may be represented in all subareas, though perhaps not to the same degree. Thus, each part of the area shows a heterogeneous petrofabric due to two tectonic events or a tectonic event incompletely overprinting a primary fabric. The separation of the subfabrics from a stereogram of the orientation distribution may then be unwise as it is difficult to separate the blend of directional variation due to differing location and that due to the competing petrofabric contributions.

In structural geology, orientation-distributions normally concern axes or undirected lines. Most natural patterns of interest disperse the directions in stretched clusters or along great circles with overall orthorhombic symmetry, for homogeneous petrofabric domains. Scheidegger (1965) described such ordered angular distributions by matrices whose three eigenvalues represent the intensity of the preferred orientation and whose eigenvectors characterize the orientations of peak, minimum and intermediate concentrations. Woodcock (1977) extended the concept of an *orientation tensor* to describe an anisotropic distribution of orientations that could range from point-cluster, through partial girdles to great circle girdles. He normalized the Eigenvalues so that their sum ($E_{\text{MAX}} + E_{\text{INT}} + E_{\text{MIN}} = 1$): point clusters have $E_{\text{MAX}} > E_{\text{INT}} \approx E_{\text{MIN}}$ and partial girdles have $E_{\text{MAX}} \approx E_{\text{INT}} > E_{\text{MIN}}$. His orientation tensor quantifies the subjective L–S scheme of Flinn (1965).

Further constraints and correspondingly more information are conveyed by structural elements that involve line-plane pairs, e.g. slickensides in fault planes, fold axes within axial planes, mineral lineations within foliations. Each linear and planar element of the pair cannot be treated separately statistically as they are integral features. If that were done, the angular relationship inherent in each line-plane combination would not be preserved in the angular relationships of their mean directions. A special treatment of such *orthogonal structural orientation data* avoids these problems (Lisle, 1989) but forms part of the more general case of *tensor statistics* discussed below (Jelinek, 1978).

Most rocks are anisotropic so that at each point in the material their physical properties such as seismic velocity, electrical conductivity, thermal conductivity or magnetic susceptibility vary, depending on the direction in which they are measured. Second-rank tensors describe the variation at a point by three magnitudes each associated with one of three, mutually orthogonal axes (Nye, 1957, p. 7). Thus, the physical property may usually be represented by a magnitude ellipsoid whose maximum, intermediate and minimum axes correspond to the principal values. To structural geologists, the *finite strain ellipsoid* is a familiar example (Ramsay, 1967). Here, however, we discuss magnetic susceptibility ellipsoids that describe the variation in magnetic susceptibility caused by low-field induced magnetization (AMS; Hrouda, 1982); or by the ellipsoid

for anisotropy of anhysteretic remanent magnetization (AARM; Jackson, 1991).

Reviewed at length elsewhere, AMS is readily measured with great precision for any rock and invariably has a direct correspondence with the orientation distribution of crystals in the rock (Fuller, 1963; Uyeda et al., 1963; Hrouda, 1982; Stephenson et al., 1986; Borradaile, 1987, 1988; Rochette et al., 1992; Borradaile and Henry, 1997). A related magnetic anisotropy that isolates the orientation distribution of remanence-bearing grains by their AARM was reviewed by Jackson (1991). AARM isolates the magnetic fabric contribution of remanence-bearing grains that usually occur as oxides or sulphides of iron or manganese. Although these occur as low-abundance accessory minerals, this subfabric may represent a different portion of the crystallization or strain history from the rock-forming minerals that contribute only to AMS. AMS combines fabric contributions from *all* minerals and it is controlled by their preferred crystallographic orientation-distributions, with the exception of magnetite whose grain-shape dictates its AMS contribution. The eccentricity of the fabric ellipsoid is most effectively described by Jelinek's (1981) P_j parameter (sphere = 1; ranging upwards with eccentricity) and its shape by T_j (+1 = oblate, -1 = prolate). An important feature of magnetic fabrics is the enormous variation in average intensity of the property. Averaging maximum, intermediate and minimum susceptibilities for a sample yields its *bulk susceptibility*, which, for most rocks, ranges from $\sim 50 \times 10^{-6}$ to $\sim 10,000 \times 10^{-6}$ SI. However, pure quartzites or limestones respond diamagnetically with a feeble bulk susceptibility $\sim 14 \times 10^{-6}$, whereas some iron formations may approach the bulk susceptibility of magnetite ($\leq 3,000,000 \times 10^{-6}$).

In a perfectly uniform substance, the AMS ellipsoids from different samples would be parallel and have principal axes of matching dimensions. For such perfectly congruent ellipsoids, any single sample ellipsoid characterizes the distribution: it represents the mean. In reality, the AMS ellipsoids vary in shape and orientation from sample to sample. Consequently, the mean AMS tensor's shape cannot be calculated as a scalar mean from the axial lengths of AMS ellipsoids. The shape of the mean tensor underestimates the anisotropy degree (P_j) and yields a shape parameter $|T_j|$ that is too close to zero (consider Fig. 1) for the individual samples because of their scattered orientations. Furthermore, in the case of magnetic petrofabrics, homogeneity is influenced not just by grain orientation-distribution but also by magnetic mineralogy because different minerals have different bulk susceptibilities, magnetic anisotropies and their proportions vary between samples.

Characterizing the mean orientations of principal directions (k_{MAX} , k_{INT} , k_{MIN}) from numerous samples is more complicated and requires the tensor-statistical approach of Jelinek (1978). Consider the non-systematic scatter of directions produced by the variability of natural processes. For a

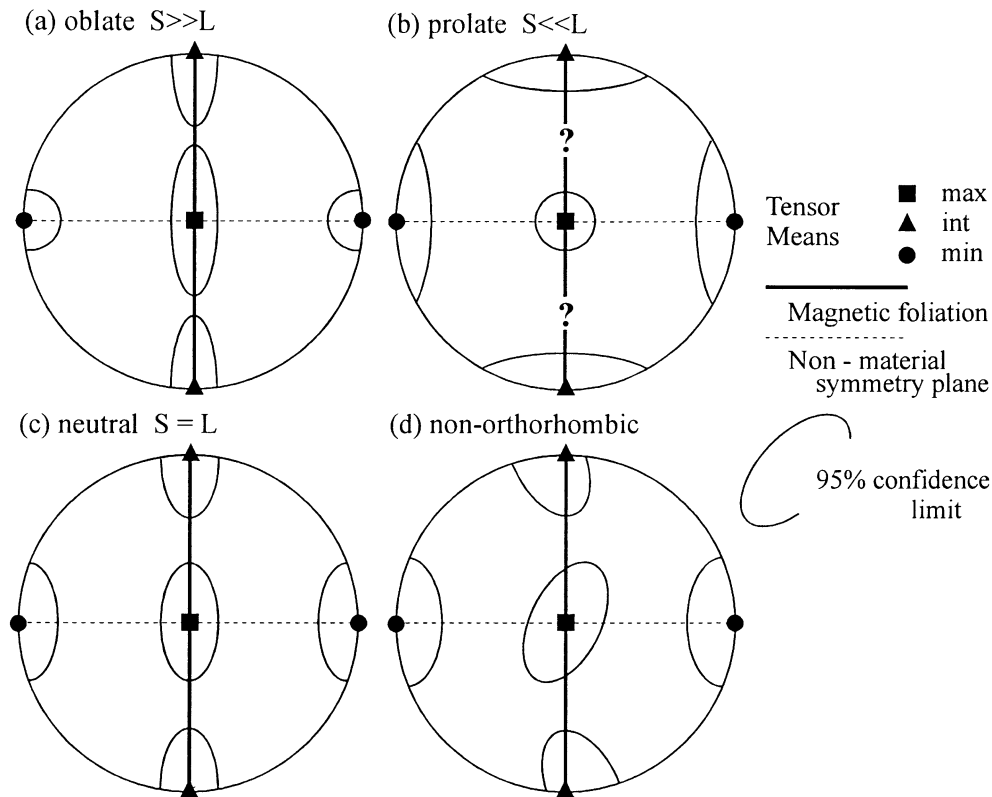


Fig. 2. Schematic lower hemisphere stereograms for idealized plots of tensor means. All subsequent stereograms in this paper are lower hemisphere, equal area projections.

single, homogeneous petrofabric this is the spherical equivalent of the linear Gaussian distribution of errors of observations. The mean anisotropy has orthorhombic symmetry with principal directions defined as maximum, intermediate and minimum susceptibilities (e.g. Fig. 2a–c). For a well-developed, simple, homogeneous petrofabric this much could be gleaned from traditional density plots (orientation-frequency distributions, e.g. Figs. 4a–c and 7a–c). The tensor-statistical calculation guarantees the constraint that the means of the principal directions are mutually orthogonal (Jelinek, 1978, pp. 52–53). Incorrectly treating AMS fabric directions as independent lines would yield false, non-orthogonal means for the three principal directions of the mean tensor. Whereas the inaccuracies of that unjustifiable procedure may be barely noticeable in the case of a saturation-alignment petrofabric due to stress-controlled metamorphic crystallization (Fig. 4d), it is normally grossly unacceptable. Thus, tensor-statistics are essential for the characterization of fabric orientation-distributions.

A further consideration in the application of tensor-statistics to magnetic fabrics arises from the enormous variation in bulk susceptibility of rocks and minerals. The orientation of the mean tensor can be distorted by the occurrence of high susceptibility minerals, an effect that can be minimized by normalizing sample-intensities (Fig. 3a and b) as recommended by Jelinek (1978, p. 53), either in a sepa-

rate subfabric or in a congruent fabric that is less abundant and poorly represented (Fig. 3). Normalizing the samples' according to their bulk susceptibility overcomes this. Examples below show that normalization is generally preferable but may lose some useful information by suppressing the identification of subfabrics that may be significant (e.g. Fig. 3c–e).

Another advantage of tensor-statistics is that they can reveal the mutual interaction of the directional uncertainty of the mean principal directions (Jelinek, 1978; Lienert, 1991). For example, the confidence cone about the mean maximum principal direction is constrained by the confidence cones about the other two mean principal directions (e.g. Fig. 2a–c). Thus, visual inspection of the elongation of the elliptical confidence cones reveals the shape of the mean tensor (e.g. $S > L$; cf. $T_j > 0$ for an individual AMS ellipsoid). In this paper, the confidence limits presented confine 95% of possible sample means. The reliability of confidence cones is restricted usually to cases where the apical angle of the cone is $\leq 25^\circ$ due to approximations in their calculation (Jelinek, 1978, p. 59). For an adequately sampled, petrofabrically-homogeneous site, the AMS-axes' confidence cones should retain orthorhombic symmetry on the stereoplot (Fig. 2a–c). This is because those constraints permit zero covariance for possible orientations of the principal axes. Subsequent case studies that demonstrate clear or reasonable orthorhombic symmetry are given in Figs. 4d,

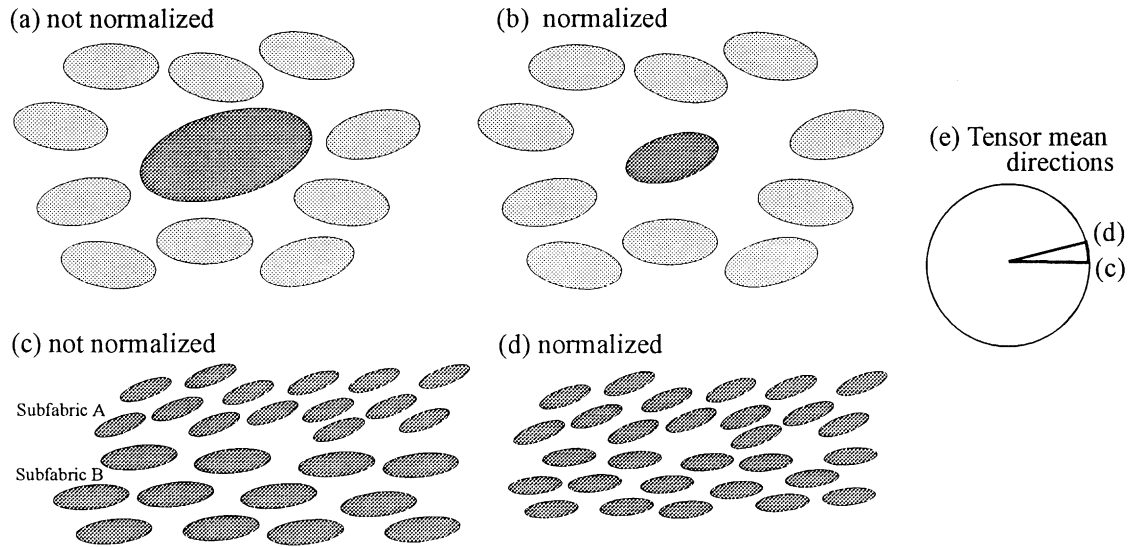


Fig. 3. The effects of normalizing samples' AMS magnitudes to suppress the influence of high susceptibility subfabrics.

5c, d, 6, 9a–c, 10a, b, 11 and 12. However, for a biased sample of a homogeneous petrofabric, or a sample-distribution comprising multiple subfabrics with different orientation distributions, it is a different matter. Where the possible orientations of all three principal axes covary, the confidence cones may have sub-orthorhombic symmetry.

It will be shown that the orthorhombic symmetry of confidence-cones may be restored or worsened by normalization of the sample-tensors magnitudes, depending on considerations of petrofabric and magnetic mineralogy. There appear to be two clear geological reasons for confidence limits to have sub-orthorhombic symmetry (e.g. Fig. 2d). First, there may be conflicting subfabrics, e.g. differing degrees of tectonic overprint on a primary fabric or asynchronous, noncoaxial tectonic subfabrics. In other words, the underlying orientation-distribution fails to achieve orthorhombic symmetry. This may even occur in a homogeneous, single-event petrofabric where the sample size is insufficient to faithfully represent orthorhombicity. Second, individual observations may derive from samples with different proportions of high-susceptibility accessory minerals. Accessory minerals may not be abundant enough to define a stable subfabric but their high bulk susceptibility may swamp the AMS contribution of the matrix. Thus, the AMS orientation of the matrix will be skewed towards that of a different or poorly represented accessory-subfabric. Of course, the latter situation is remedied where each sample's tensor is normalized by its bulk susceptibility value although that procedure may also suppress some useful information (Jelinek, 1978, p. 53), as discussed below.

Strictly speaking, markedly non-orthorhombic confidence limits indicate that the sample-distribution is unfavorable for treatment by Jelinek's statistical approach. On the one hand, we may be treating an ideal orthorhombic,

unimodal population-distribution that has been inadequately sampled, a common and insurmountable problem in field geology. On the other hand, the underlying population-distribution may be multimodal. Nevertheless, whichever the case, Jelinek's statistics are useful as they alert one to either of the two possibilities. In particular, bimodal distributions are commonly subtle but sensitive to detection by Jelinek's asymmetric confidence cones. Moreover, stereographic inspection of orientation distributions usually provides the first opportunity to detect multiple petrofabric events. Therefore, cautious use of Jelinek's tensor statistics is justified even if the sample-distribution does not rigorously satisfy their precise requirements.

The approach here is to examine seven case studies of magnetic fabrics that summarize the orientation distribution of minerals metamorphic, igneous and sedimentary rocks. Anisotropy of low field susceptibility (AMS) is used in all cases, but the orientation-distribution of magnetite was isolated by anisotropy of anhysteretic remanence (AARM) in three case studies. Each study indicates some strength or pitfall of interpretation of the orientation distribution of a sample of tensors, and each is peculiar to the case in hand. Provided we inspect and respect the idiosyncrasies of each sample, the symmetry and normalization procedures for the sample may reveal useful new information concerning fabric heterogeneity and multiple fabrics as well as the traditional information about the shape and orientation of the mean fabric ellipsoid.

2. Case studies

2.1. Borrowdale Volcanic Group Slates, English Lake District (Fig. 4: $n = 74$)

This sample of 74 cores from a study by Borradaile and

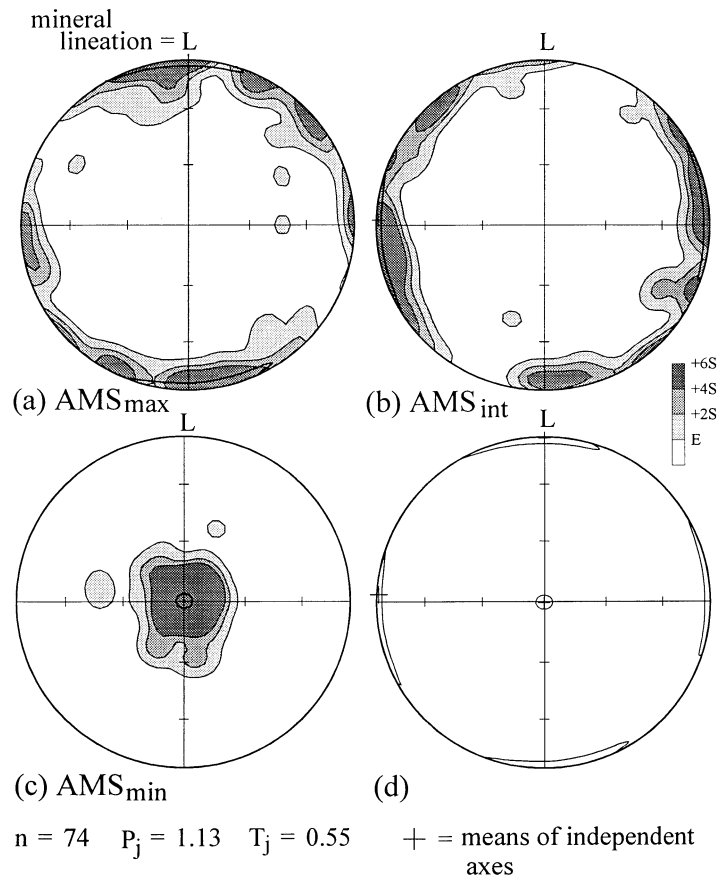


Fig. 4. Borrowdale Volcanic Group slates of Northern England. The samples are oriented with reference to their slaty cleavage in the horizontal and their fabric structural lineation N–S. The latter is defined by stretched volcanic lapilli and a chlorite mineral lineation. All other case studies in this paper orient the samples in geographic coordinates. (d) Shows fortuitous correspondence between mean orientations of principal susceptibilities calculated as though they were independent axial directions and by tensor-statistics. The almost perfect orthorhombic symmetry of the tensor means' 95% confidence limits is due to the strong preferred orientation.

Mothersill (1984) are plotted in a fabric orientation-coordinate system with the prominent mineral lineation of chlorite and stretched volcanic lapilli arbitrarily oriented N–S, and the slaty cleavage horizontal. (In all other case studies, the samples are in geographic coordinates.) The AMS fabric is oblate with a well-defined k_{MAX} lineation and a moderately well-defined oblate symmetry, as shown by the similarly developed elongated girdles for k_{MAX} and k_{INT} . (Fig. 2a and b). The principal susceptibilities for each sample are individually contoured at multiples of the expected density 'E' of a hypothesized equivalent normal distribution, shown in the legend as E, 2E, etc. (Spheristat Commercial software; Pangea Scientific).

Chlorite and magnetite control AMS in the Borrowdale volcanic slate (Borradaile and Mothersill, 1984; Nakamura and Borradaile, 2001). However, chlorite dominates AMS, and it possesses a near-saturation crystallization fabric. The strain history is essentially coaxial so that the bimodal magnetic mineralogy and single penetrative deformation produce orientation distributions of the principal susceptibilities that conform well to orthorhombic symmetry (Fig. 4a–c). Consequently, there is a fortuitous corre-

spondence between the mean principal AMS directions calculated from tensor statistics with the mean directions considering the samples' principal susceptibilities as independent axial directions (Fig. 2d). Similarly, the subhorizontal magnetic foliation defined by the mean-tensor $k_{MAX} - k_{INT}$ is almost indistinguishable from the independently calculated axial-directions (Fig. 4d). The orientations of mean principal susceptibilities defined by tensor-means and axial-direction-means differ by $<2^\circ$ in this case.

The confidence cones of the tensor-mean principal directions show well developed orthorhombic symmetry, extremely elongate in the magnetic foliation ($k_{MAX} - k_{INT}$) and a tight cluster defining the confidence about k_{MIN} . This is characteristic of the strongly oblate, slaty fabric. However, the scalar-mean shape of AMS ellipsoids ($T_j = 0.55$) misleadingly underestimates the oblateness of the orientation-distribution. The shapes or symmetry (T_j) of the mean anisotropy ellipsoid and the fabric-ellipsoid defined by the orientation-distribution of the axes are different concepts (e.g. Fig. 1). Invariably, the prolateness or oblateness of an AMS orientation distribution is less extreme than that of the constituent sample-ellipsoids. For example, even if

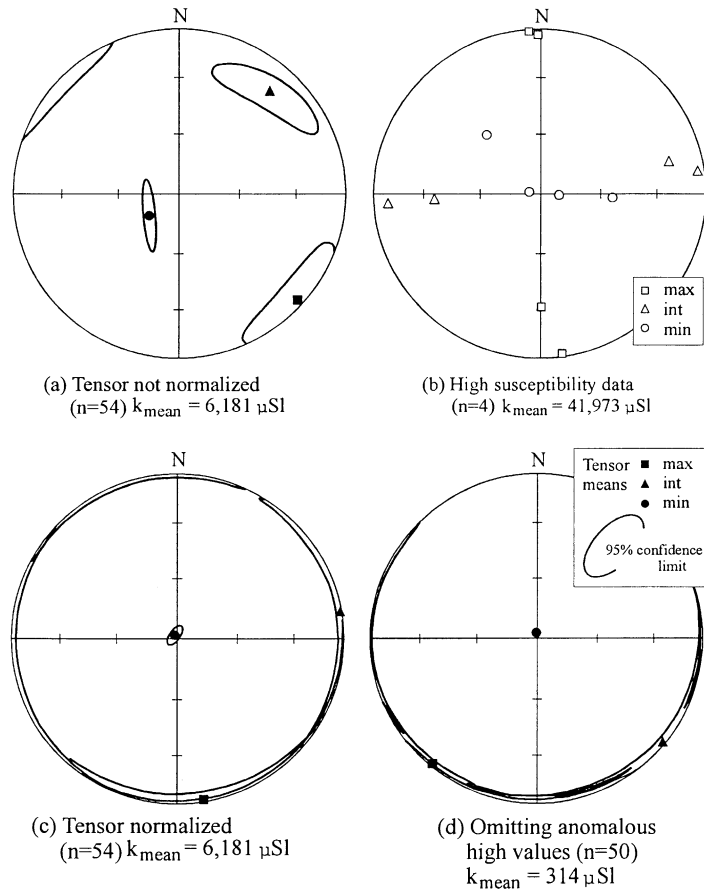


Fig. 5. AMS fabrics for slates (Otago 'schists', near Dunedin, New Zealand). The orientations of the tensor means is different for samples whose tensors are not normalized (a) or normalized (c). In this case, the differences can be attributed to four anomalous samples (b) whose exclusion produces a much clearer picture of the strong fabric and symmetry of these schists (d).

the individual minerals had $T_j = -1$, the orientation distribution of a sample of specimens would have T_j closer to zero, due to the scatter imposed by the controlling L–S fabric. Furthermore, *prolate* AMS sample-ellipsoids may be scattered in a plane to yield an orientation-distribution of AMS axial-directions that is *oblate* (S-tectonite; $T_j \sim +1$). Conversely, oblate AMS sample-ellipsoids may be scattered to share a zone axis yielding a prolate orientation-distribution of axial directions (L-tectonite; $T_j \sim -1$)

2.2. Otago schists, near Dunedin, New Zealand (Fig. 5: $n = 54$)

In the introduction, reference was made to the benefits of normalizing individual tensors to facilitate the identification of the orientation of the mean tensor for the sample-distribution. This is most dramatically revealed where a small number of the samples have both anomalously high susceptibility-magnitudes and atypical orientations. Where one disregards the actual magnitudes of susceptibility, a few sample ellipsoids of large magnitude (individual sample- P_j) and unusual orientation bias the mean tensor orientation for the sample-distribution. The orientation tensor mean of the

majority of samples is skewed towards the orientation of the anomalous samples, or 'outliers'. Jelinek recommended normalizing sample-tensors by their bulk-susceptibility to diminish the contribution of outliers. Thus, the principal directions of individual AMS ellipsoids are weighted equally, reducing the emphasis given by the AMS of high susceptibility samples. However, from the outset we should not assume that high- k outliers must be discarded: in the context of a particular study they could be significant.

The mean tensor and confidence limits for the orientation-distribution of 54 non-normalized AMS sample ellipsoids of Otago schist samples define an orthorhombic L = S orientation distribution, shown by similarly elongate confidence ellipses about k_{MAX} and k_{INT} that also define a foliation dipping gently NE (Fig. 5a). Four samples have anomalously high susceptibility (mean = 41,973 μSI) with principal directions that are also aberrant (Fig. 5b).

Normalizing either all the sample ellipsoids (Fig. 5c), or those excluding the four outliers (Fig. 5d) defines a horizontal foliation with a tight confidence cone about k_{MIN} and very elongate cones for k_{MAX} and k_{INT} parallel to foliation. This conforms well to the field observations of a subhorizontal, well-defined schistosity with a flattening fabric ($S \gg L$). Thus, normalizing has clear benefits in this

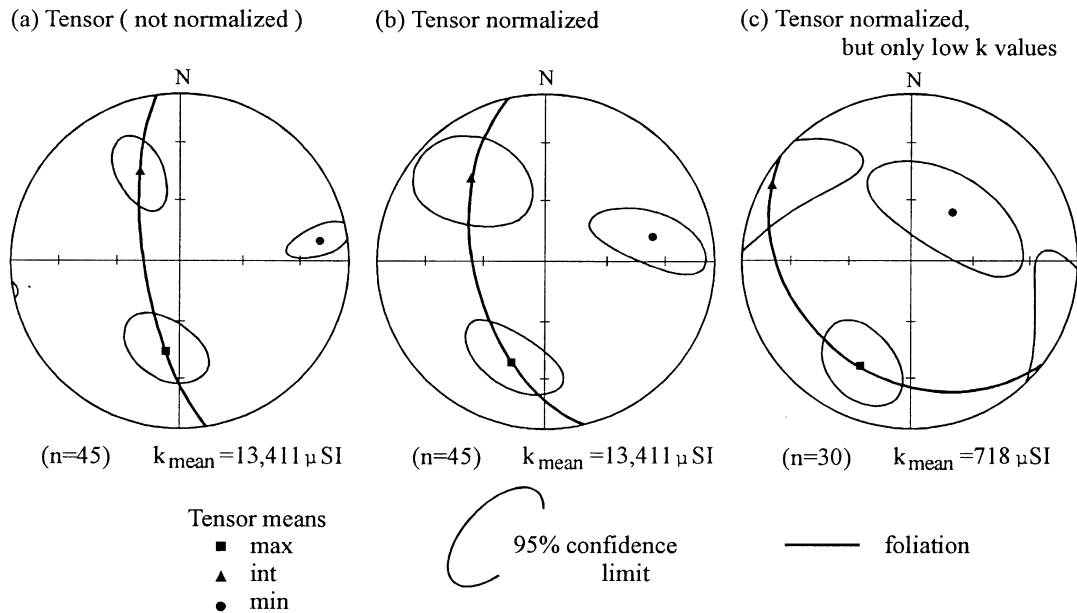


Fig. 6. Medium-grade schists, Southland and Milford Sound areas, New Zealand. (a, b) poor orthorhombic symmetry of the AMS orientation-distribution, regardless of normalization. (c) Exclusion of a high susceptibility subfabric reveals a differently oriented magnetic fabric with clear orthorhombic symmetry.

case. However, at a more subtle level, the exclusion of the four outliers considerably changes the interpretation of the k_{MAX} -orientation (mineral- or extension-lineation). The k_{MAX} is no longer south directed (Fig. 5c) but clearly south-west (Fig. 5d).

2.3. Medium-grade Schists, Southland–Milford Sound, New Zealand (Fig. 6: $n = 45$)

The AMS orientation-distribution of these schists is not well defined. Whether we normalize (Fig. 6a) or do not normalize (Fig. 6b) the samples' bulk susceptibilities, the orientations of the mean tensor are similar with a moderately steep ESE-dipping foliation and SSW k_{MAX} lineation. However, in neither case do the confidence cones inspire orthorhombic symmetry. This alerts us to the possibility of multiple magnetic subfabrics. Indeed, the magnetic mineralogy is quite complex, with several minerals of similar susceptibility and strong anisotropy competing for control. Minor variations in their proportions between samples, or in their individual orientation-distributions could account for the sub-orthorhombic symmetry. As an example of an initial interpretation, one notes that bulk susceptibility of all samples has an average value of $13,411 \mu\text{SI}$; greatly exceeding the maximum susceptibility of any paramagnetic silicate ($\sim 2000 \mu\text{SI}$). This is due to the contribution of several iron-accessory minerals as well as high-susceptibility, high-anisotropy silicates. Isolation of a sub-sample of 30 sites with much more closely grouped mean susceptibilities, averaging $718 \mu\text{SI}$, yields a mean tensor with whose confidence cones have recognizable orthorhombic symmetry (Fig. 6c). However, the magnetic foliation is now SW-dipping

compatible with structural observations, and probably confirming the presence of multiple magnetic subfabrics. The elongation of the confidence cones for k_{MIN} and k_{INT} towards one another and an almost circular confidence cone for k_{MAX} , favor a linear component to the orientation-distribution of this subset of AMS ellipsoids. The orientation-distribution's fabric ellipsoid is therefore of the $L > S$ type, tending to an L-tectonite (L), despite the average sample-AMS ellipsoid being disc-shaped, or tending to oblateness ($T_j > 0$).

2.4. Rainy Lake schistose anorthosite, Archean, Canada (Figs. 7 and 8: $n = 161$)

This sample set provides AMS measurements from a large anorthosite body with moderately high susceptibility ($k_{\text{MEAN}} = 8251 \mu\text{SI}$). AMS is controlled by magnetite shape orientations and by the preferred crystallographic orientations of mafic silicates (Borradaile et al., 1998). Outcrops reveal a feebly-developed, unstably-oriented schistosity in outcrop, largely due to the coarse grain-size and absence of phyllosilicates. The schistosity is a spaced, partly cataclastic foliation. For similar reasons, the AMS fabric is not strongly developed (Fig. 7), but there is the added complication that it is difficult to determine site-representative AMS from 10.5 cm^3 cores of such coarse-grained plutonic rocks. Multiple cores per sample only partially alleviate this problem. The density distributions that have poorly-defined contour levels are poorly defined with k_{MIN} defining an approximate NE–SW vertical foliation (Fig. 7c) and a steep SW-plunging k_{MAX} defining the mineral-lineation in the foliation plane. The mean tensor for the orientation distribution has rather circular confidence cones about the

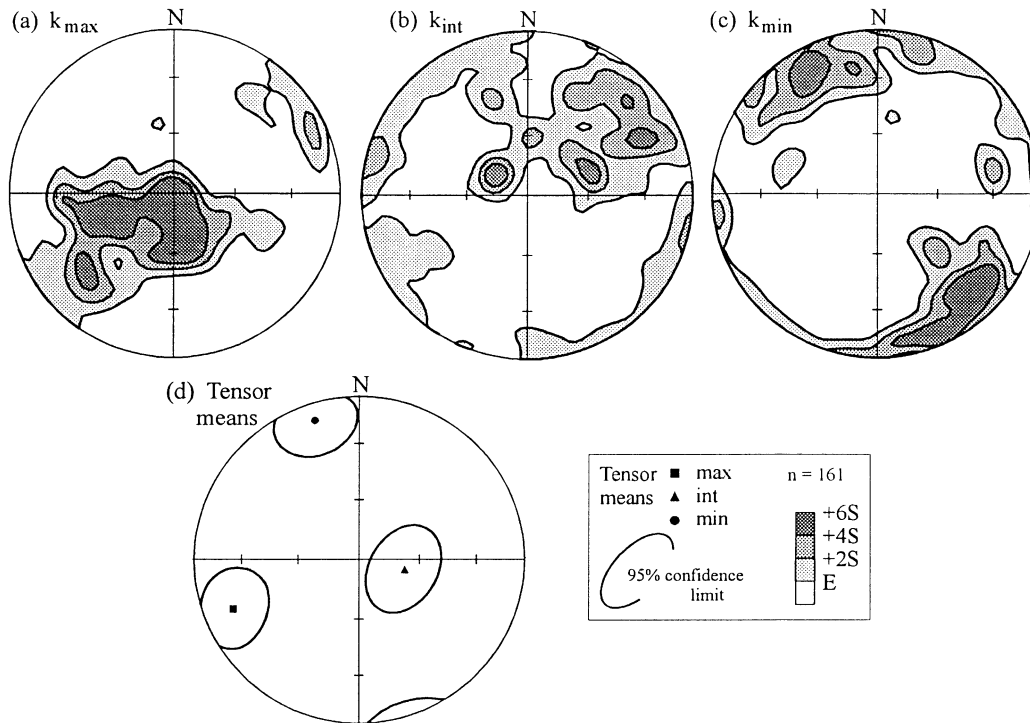


Fig. 7. An Archean anorthosite at Rainy Lake, Northern Ontario, shows poorly developed field fabrics although AMS orientation distributions reveal a modest deformation petrofabric.

mean-principal directions associated with an $L \approx S$ type fabric.

The samples possess a multi-modal magnetic mineralogy and multimodal frequency-distributions of susceptibility. Therefore, it is appropriate to compare mean-tensors for all samples, high-susceptibility outliers and the majority of samples that exclude outliers (Fig. 8). The effects of normalization of samples according to their bulk-susceptibility is then also considered.

The entire suite of samples reveals a mean tensor whose orientation could be approximately predicted from the density-distributions; its confidence cones are somewhat sub-orthorhombic (Fig. 8a). However, in this study, normalization yields a meaningless fabric, unrelated to the actual AMS orientation distributions or field-foliation (Fig. 8b). A sub-sample of 20 was identified with a bulk-susceptibility of $125,970 \mu\text{SI}$, 15 times greater than the mean for the sample-suite. The non-normalized and normalized mean-orientation tensors for the outliers are shown in Fig. 8c and d. In each case, the orientations of the principal directions are similar to those of the entire suite, indicating their strong contribution to the entire sample. However, the confidence cones are non-orthorhombic, perhaps due to unrepresentative sampling ($n = 20$) or a multi-modal subfabric within the high susceptibility outliers. Removing the high susceptibility outliers from the suite produces the orientation distributions that conform best with geological observations, have the tightest confidence cones, and improved orthorhombic symmetry (Fig. 8e and f). Imperfect ortho-

rhombicity indicates the persistence of complications due to magnetic mineralogy or multiple fabrics, and normalization does not appear to have any benefit (Fig. 8f).

2.5. Magmatic versus tectonic fabrics: Late Archean granitic plutons, N. Ontario (Fig. 9: $n = 75$, $n = 48$)

Cross-cutting relations and thermal-aureoles indicate that two small, equidimensional, Archean granitic plutons are post-tectonic. Moreover, the orientations of their megacrysts define a concentric foliation, following the intrusions' contacts, compatible with the hypothesis of magmatic inflation. However, the AMS foliations and lineations within the granites are sub-parallel to the schistosity and mineral lineation of the encasing schists (Borradaile and Kehlenbeck, 1996). This was explained by reactivation or continuation of the regional stress-field after intrusion, imposing a 'tectonic' fabric on the multi-domain magnetite by domain-wall rearrangement. The orientation of the mean tensor and its confidence limits for normalized and non-normalized sample-tensors of the Trout Lake and Barnum Lake plutons are shown in Fig. 9a and b and c and d, respectively. The mean susceptibilities for both plutons are high (Trout Lake pluton, $k_{\text{MEAN}} = 27,307 \mu\text{SI}$; Barnum Lake pluton, $k_{\text{MEAN}} = 15,404 \mu\text{SI}$), their AMS being controlled primarily by multi-domain magnetite, with negligible contributions from mafic silicate. The initial approach is to calculate the mean tensor from normalized samples, since one would expect to clarify the dominant

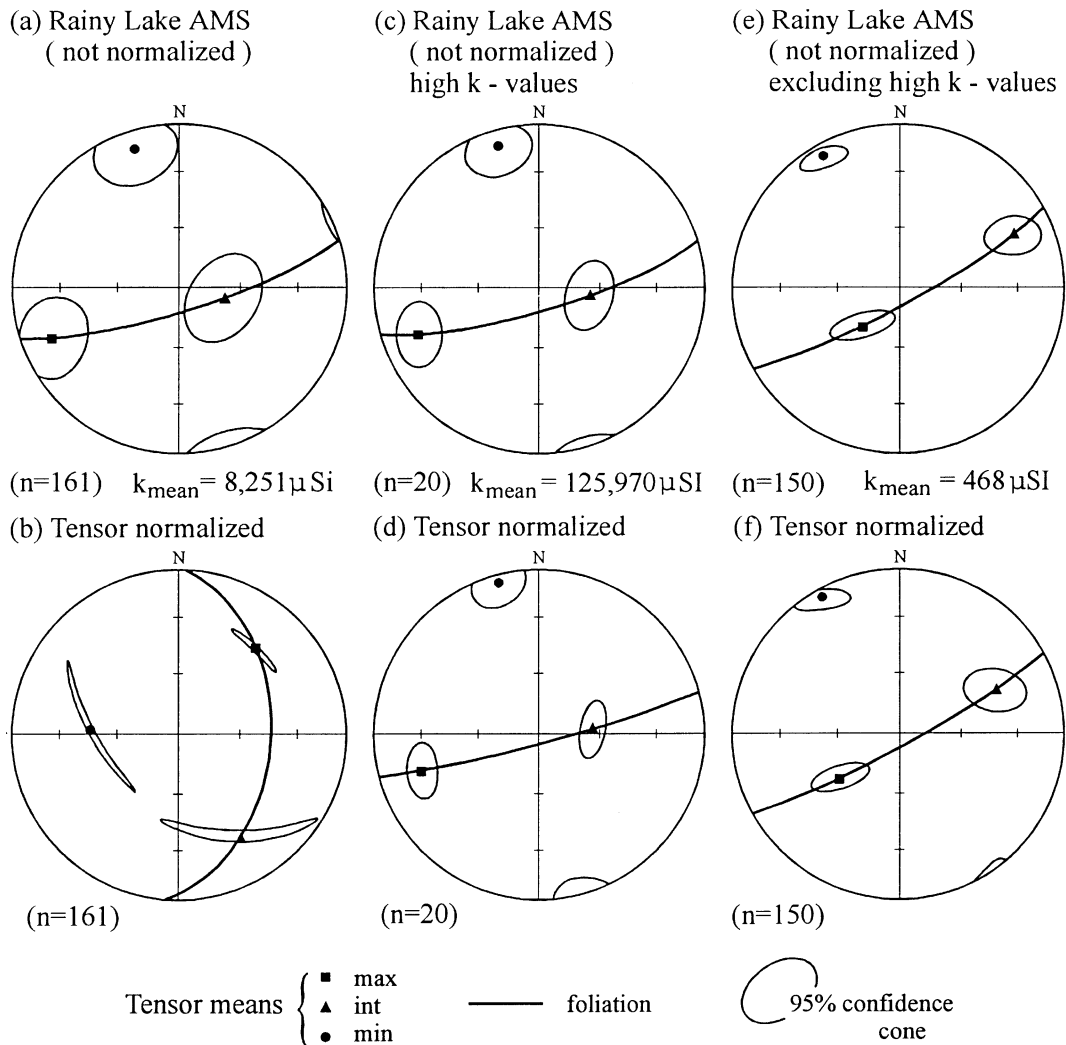


Fig. 8. Archean anorthosite, Rainy Lake, Northern Ontario. (a, b) Normalization does not improve the definition of the tensor mean for the entire sample. (c, d) Twenty extremely high susceptibility samples appear to dominate the raw data-set, of (a). (e, f) Exclusion of high susceptibility outliers yields a data set with similar mean directions, confidence cones and orthorhombic symmetry for both normalized and non-normalized sample tensors.

magnetite-fabric. This demonstrates clear orthorhombic-symmetry for the mean AMS tensor (Fig. 9a and b), that can only be of post-intrusion origin because it is congruent with country rock fabrics. The symmetry of confidence ellipses for the Trout pluton define an S-fabric, whereas those for the Barnum pluton imply an $L \approx S$ fabric, although both have similar foliations and lineations (Fig. 9a and b).

What are the respective values of normalizing or failing to normalize such data? In an AMS fabric dominated by magnetite, as here, the advantages of normalization might be expected because they would smooth the variations in magnetite content, whose grain-anisotropy is weak but bulk susceptibility is high. This is revealed when we inspect mean tensors for non-normalized samples (Fig. 9c and d) because these show less perfect orthorhombic symmetry of the confidence cones. Nevertheless, both normalized and non-normalized samples yield similarly oriented mean-tensors.

The non-normalized samples from the Trout Lake pluton (Fig. 9c), have very similarly oriented tensor-means and confidence cones to the normalized samples; one minor difference is that the magnetic foliation is slightly shallower dipping for non-normalized tensors. However, for the Barnum Lake pluton (Fig. 9d), there are some changes in the shape of the confidence cones for k_{INT} and k_{MIN} ; they are elongated in the plane perpendicular to k_{MAX} indicating that the orientation-distribution has a stronger linear component ($L > S$) than for normalized samples that have $L \approx S$. Clearly, the non-normalized samples preserve the weighting of high susceptibility samples that carry a stronger L-component. The petrofabric interpretation of these features is open to debate but one possibility is that the high susceptibility samples record a different aspect of the strain history, e.g. an earlier or a later part or a longer time-span than lower susceptibility samples. These samples, and the special tectonic or magmatic effects that they represent,

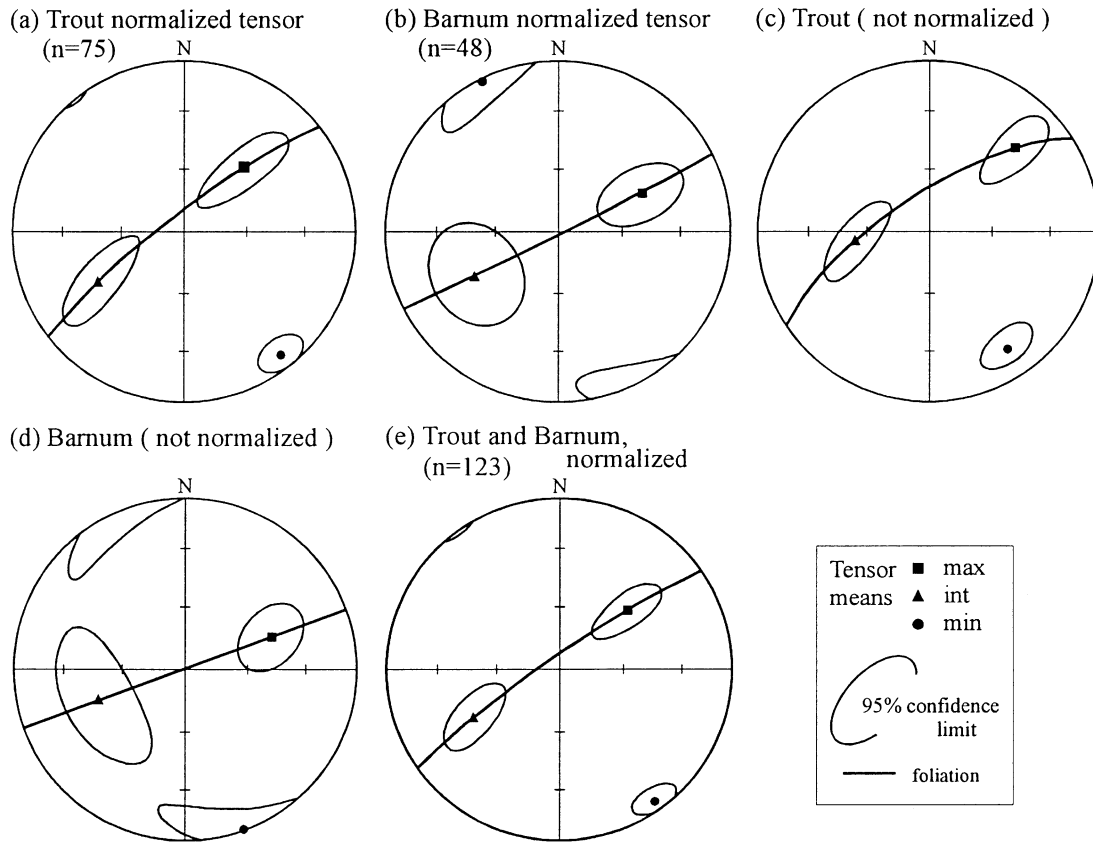


Fig. 9. Two post-tectonic late Archean granites, Northern Ontario. (a, c) Normalization of the sample tensors for the Trout Lake granite little changes the tensor statistics that indicate L = S orientation-distributions for AMS principal directions. (b, d) Normalization for the Barnum Lake pluton reduces the bias due to some high-susceptibility outliers making the statistics similar to those for the normalized samples. (e) Stacked data from both plutons improves the definition of tensor-statistics (tighter confidence cones); this validates the use of tensor statistics to confirm petrofabric homogeneity of distinct 'subareas' (here separate plutons).

feature more prominently in tensor means from non-normalized samples. Thus, again we see an advantage of tensor-means and orientation distributions derived from non-normalized sample-AMS.

This case study provides another useful test and use of the benefits of tensor-statistics. The two 'sites', represented by the two plutons are geologically coeval, but quite separate lithological units. They are the most distinct example of subareas that should be petrofabrically homogeneous; a situation analogous to adjacent subareas in a regional structural study. This is confirmed by combining the two data sets and calculating their overall mean tensor. For the purposes of illustrating this point, only normalized sample-AMS is used (Fig. 9e). Because the two intrusions represent congruent petrofabric domains, the stacked data yield a mean tensor plot with smaller confidence cones, better-defined orthorhombic symmetry and closer correspondence with the country rock fabrics than the individual bodies (Fig. 9e). Of course, the subtle differences in L–S symmetry (cf. Fig. 9a and b) are lost due to data-stacking but the advantage is that the definition of the mean-tensor is enhanced and where that occurs, the congruity of the stacked domains is confirmed.

3. Case studies involving two fabrics determined from AMS and AARM

The preceding examples revealed subtleties in the characterization of a sample of imperfectly aligned AMS ellipsoids. AMS blends the contributions of *induced* magnetization from all minerals; diamagnetic, paramagnetic and remanence-bearing. Consequently, each individually measured AMS tensor merges several different AMS orientation-distributions: one for each mineral present within the sample! For medium-grained and finer samples there are normally enough grains of each mineral to provide a representative orientation-distribution contribution for any of the minerals in the rock.

Although the *remanence*-bearing minerals are normally accessories, present as a few percent of the sample-volume, their susceptibility may dominate the AMS signature, especially in the case of magnetite, titanomagnetite or pyrrhotite. Fortunately, their ability to retain a record of the induced field after its application means that we can isolate their orientation-distribution from a separate experiment that measures anisotropy of remanence (AARM; Stephenson et al., 1986; Jackson, 1991). The anisotropy of

remanence is normally measured from anhysteretic remanence (ARM) as an AARM, although anisotropy of isothermal remanence may also be successful with careful choice of applied fields (Daly and Zinsser, 1973; Borradaile and Dehls, 1993; Jelinek, 1993; Dunlop and Özdemir, 1997). Unfortunately, because of the different physical response of the *same mineral* to remanent and induced magnetism, its AARM and AMS tensors always differ in shape and may differ in orientation (Stephenson et al., 1986; Jackson, 1991; Rochette et al., 1992). Therefore, we cannot simply subtract the accessory-AARM contribution from a sample's AMS to isolate the matrix-AMS. Convolved and sometimes unreliable methods have been developed to attempt this, but it is not recommended as a routine approach (Borradaile et al., 1999a; Hrouda et al., 2000). Nevertheless, orientation-distributions of AARM and AMS may be compared qualitatively to assess the relative contributions of the matrix of primary rock-forming minerals and the normally younger accessory minerals. This adds a temporal element to the petrofabric interpretation from which noncoaxial strain histories and shear-sense may be detected (e.g. Borradaile and Henry, 1997). Applying tensor statistics raises comparisons beyond the qualitative level. It should be noted that the orientation-distribution of certain accessory minerals may be more easily identified from the anisotropy of complex-susceptibility (electrical conductivity), for example pyrrhotite (Borradaile et al., 1992).

The following case studies compare the application of tensor statistics for AMS and AARM data from the same samples. Unfortunately, the sample-requirements for a successful AARM determination are more demanding than those for AMS measurement. Consequently, for most sample-suites as few as 25% of the AMS samples yield reliable AARM data. This makes statistical comparisons somewhat uneven, unless further sampling specifically equalizes the number of AARM and AMS measurements, as in the first of the following case studies. In my experience of re-sampling, as long as $n > 50$ for any reasonably well-defined orientation distribution of either AMS or AARM, the benefits of further measurement risk the law of diminishing returns. The same is not true for structural directions or paleomagnetic vectors: sampling-demands seem to be eased at a practical level for tensors that have the added internal constraints of orthorhombic, three-axis symmetry.

3.1. Kapuskasing Structural Zone, Canada (Figs. 10 and 11: $n = 60$, $n = 77$)

The Kapuskasing structural zone of Northern Ontario thrusts up granulite facies gneisses of the Archean lower crust. The field schistosity and lineation are expressed poorly in outcrop due to the weak dimensional anisotropy of the pyroxenes, feldspars and garnet. However, AMS and AARM reveal consistent, well-defined orientation distribu-

tions over areas of tens of square kilometres (Borradaile et al., 1999b). AMS is defined by mafic silicates and magnetite, AARM is defined by the magnetite-subfabric.

Without normalizing sample-tensors, the mean tensor and confidence cones define subhorizontal, ENE–WSW, linear fabrics for both AMS and AARM (Fig. 10a and b). This is evident from k_{INT} and k_{MIN} confidence cones elongate in the plane perpendicular to k_{MAX} , typical of an $L \gg S$ tectonite. (Note that the scalar-averaged sample shapes for AMS and AARM have $T_j = 0.01$ and 0.22 , respectively; quite unrelated to the ‘shape’ of their orientation-distribution tensor.) The AARM dispersion is greater and its k_{MAX} lineation plunges slightly WSW. The confidence cones for the respective principal axes of AMS and AARM barely overlap, identifying a separate magnetite-subfabric, probably due to minerals growing over during a protracted noncoaxial strain history. AMS is influenced both by silicates and magnetite, whereas AARM isolates the younger magnetite subfabric. Therefore, comparison of Fig. 10a and b suggests that the strain history was non-coaxial. Although the logic of normalizing is to weigh all samples’ fabric directions equally, for a bimodal mineralogy or bimodal petrofabric, non-normalized tensors preserve the importance of high-susceptibility samples.

The mean tensor for normalized sample-anisotropies is shown in Fig. 10c and d. The principal directions are now differently oriented; and the k_{INT} and k_{MIN} confidence cones are more circular, compatible with an $L \approx S$ fabric. This is also true of AMS and AARM, although AARM foliations are differently oriented. In light of our knowledge of regional geology (Borradaile et al., 1999a,b), the normalized AMS samples have a misleadingly oriented mean tensor. However, the mean tensor for normalized sample-AARM clarifies the contribution of magnetite alone and correctly reveals the field-foliation, which is also a cryptic seismic reflector (Borradaile et al., 1999a,b). Therefore, one sees benefits from the use of both normalized and non-normalized sample anisotropies. Superposition of tensor-mean data for the most appropriately and equivalently treated data, in this case non-normalized samples, graphically clarifies the degree and sense of noncoaxiality in strain history (Fig. 11). This is not quite the same kind of ‘data-stacking’ used in the previous section (cf. Fig. 9e) as the anisotropies record different magnetic phenomena (AMS: AARM), but the concept of data stacking provides an added interpretive tool, combined with normalization/non-normalization in the application of the tensor statistic.

3.2. Mantle Lherzholites, Troodos Ophiolite, Cyprus (Fig. 12: $n = 400$, $n = 111$)

The doming of central Cyprus exposes a formerly sub-oceanic, upper mantle sequence of harzburgites grading upwards through a dike complex to pillow lavas. The mantle-sequence harzburgites have frequency distributions of bulk susceptibility with two modes, corresponding to

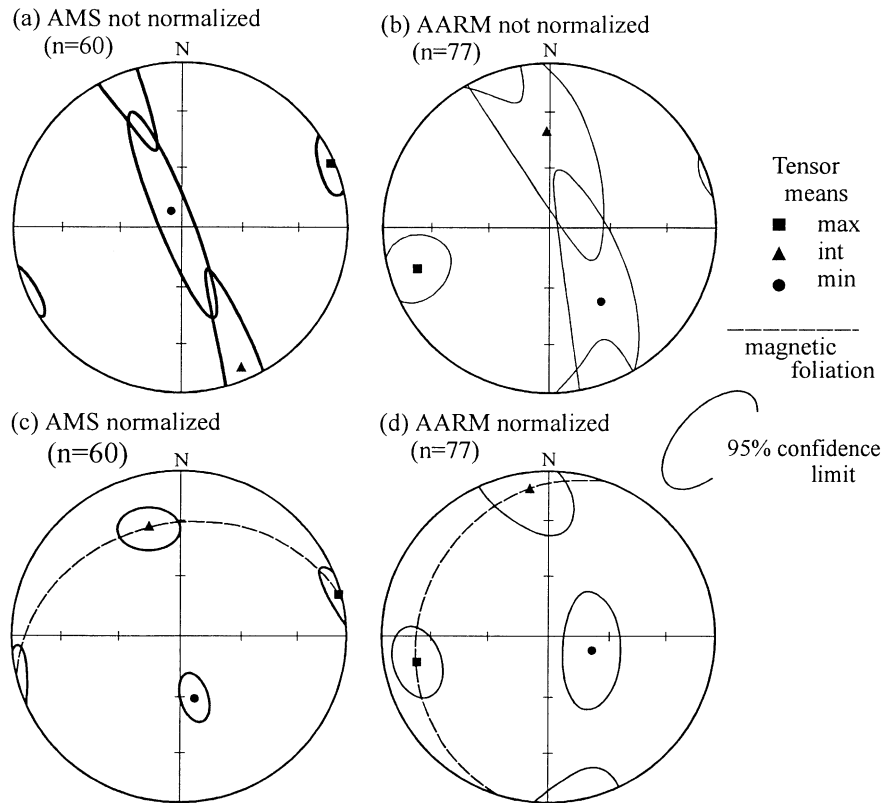


Fig. 10. Kapuskasing Zone, lower crustal Archean granulitic gneiss, in northern Ontario, Canada. (a, c) Normalization of AMS sample tensors changes symmetry estimates of average principal orientations and tightens confidence cones and produces results incompatible with our knowledge of regional geology and kinematics. (b, d) Normalization of the AARM fabric, however, identifies a magnetite subfabric whose orientation and significance are compatible with field structures and regional kinematics.

contributions from mafic silicates, chromite, magnetite and ilmenite. The magnetic fabrics were used in a regional fabric study to determine the solid-state flow patterns during the emplacement and serpentinization of the harzburgite (Borradaile and Lagroix, 2001).

Without normalizing sample-AMS, the mean tensor of the AMS orientation-distribution has nicely orthorhombic symmetry of the $S > L$ type, as shown by circular confidence cones for k_{MIN} but elongate elliptical cones for k_{MAX} and k_{INT} , parallel to the magnetic foliation (Fig. 12a). This concurs with field observations of macroscopic mineral foliation and lineation. However, when the tensors are normalized, the contribution of the high susceptibility accessory minerals is suppressed and conflicting contributions from mafic silicates become significant. This lessens the correspondence with the field measurements and confidence cones are expanded (Fig. 12b). Here, normalization lessens the definition of the mean tensor for the AMS orientation-distribution.

In contrast, AARM is dictated by the magnetite, although more than one magnetite subfabric is present. Thus, the mean tensor for non-normalized samples has poorly developed orthorhombic symmetry, with k_{MAX} and k_{INT} confidence cones oblique to the magnetic foliation (Fig. 12c). Normalization of this mono-mineralic fabric weights

the contribution of individual sample-tensors equally so that influences of different magnetite subfabrics merge, restoring orthorhombic symmetry (Fig. 12d). In this example, the statistical characterization of the AMS fabric does not benefit from normalization, whereas the AARM fabric does. Clearly, each case must be evaluated on its own merits.

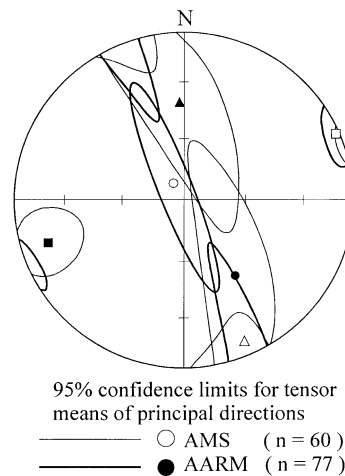


Fig. 11. Comparison of mean tensors for AMS and AARM, Kapuskasing Zone granulite gneisses, Northern Ontario, Canada.

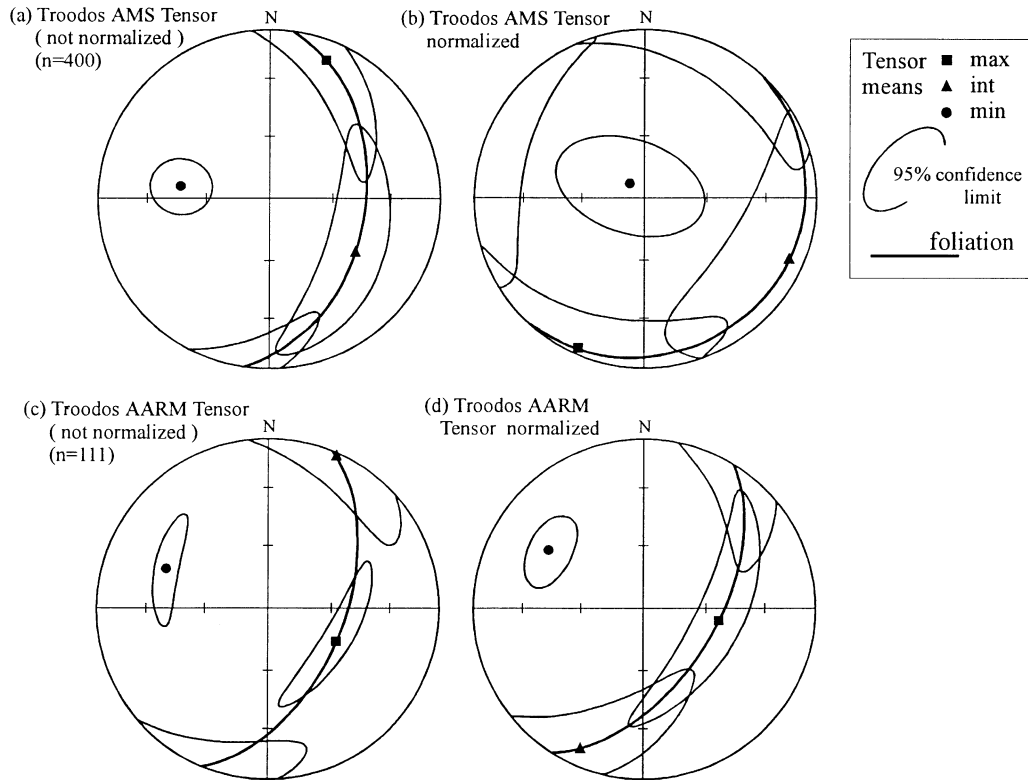


Fig. 12. Comparison of AMS and AARM and the effects of normalization of the sample tensors, for the Troodos mantle sequence harzburgites of Cyprus. (a, b) Normalization of AMS reduces the dominant signal from the magnetite subfabrics: consequently, normalization produces a spurious fabric with poorly expressed orthorhombic symmetry. (c, d) Normalization of AARM, in contrast, improves the signal of a single (magnetite) subfabric by reducing the weight of anomalous high susceptibility outliers.

4. Conclusions

Traditionally, petrofabrics, structural directions and magnetic fabrics were evaluated by visual inspection of contoured stereogram density plots. Since magnetic fabrics are represented by second-rank tensors, contours of all three axes of each sample tensor are required to fully describe the orientation distribution. It is wiser always to plot all three axes (e.g. Lienert, 1991) to fully appreciate the orientation-distribution. The clustering or girdling of each of the maximum, intermediate and minimum axes may designate the shape of the fabric ellipsoid, qualitatively, in the L–S scheme of Flinn (1965). This requires judgement and experience because the density plots lack the perfect orthorhombic symmetry of the individual sample ellipsoids, but structural geologists are familiar with interpreting *orientation-distributions* by this procedure. The study of the cases presented yields the following conclusions:

1. The *shape* of the ellipsoid describing the orientation distribution (L, $L > S$, $L = S$, etc.) is unrelated to the mean *shape* parameter, (usually described by T_j) of individual sample-AMS ellipsoids. The orientation-distribution ellipsoid's shape underestimates the shape of the average AMS-ellipsoid, and its

symmetry (e.g. prolateness or oblateness) may be quite different.

2. Confidence limits about the orientations of the mean tensors' principal directions may have imperfect orthorhombic symmetry. Geological reasons for this could include multiple mineralogical sources of magnetic anisotropy, minerals having both different bulk susceptibilities and anisotropies, or multiple magnetic subfabrics (Hrouda, 1982; Borradaile and Mothersill, 1984; Borradaile 1987, 1988, 1991; Henry, 1989; Hrouda and Schulmann, 1990; Borradaile and Henry, 1997; Hrouda and Jelinek, 1999; Hrouda et al., 2000; Lacroix and Borradaile, 2000). One must always distinguish the competing roles of anisotropy and bulk susceptibility. A mineral or subfabric of low anisotropy but high magnetic susceptibility may mask contributions from more weakly anisotropic sources and vice versa. For example, the AMS orientation-distribution of one or more rock-forming silicates may compete with low-abundance, highly susceptible accessory iron-minerals. The same complexity exists for AARM, which may blend multiple subfabrics of remanence-bearing accessory minerals.
3. Accessory minerals may be too few to define a stable subfabric but their high bulk susceptibility may swamp

the matrix's AMS contribution. Thus, the matrix-AMS orientation will be skewed towards that of a different, or poorly represented, accessory-subfabric.

4. Jelinek's normalization procedure decreases the contribution of high-susceptibility outliers, rendering each sample the same weight. This may improve the degree of orthorhombic symmetry of the confidence limits. However, in some cases, normalization worsens the symmetry of confidence limits. The benefits of normalization depend on complex considerations of magnetic mineralogy, including the bulk susceptibilities and anisotropies of each mineral, as well as the orientation-distribution of each mineral.
5. Normalization should be applied to the entire sample, as well as a sub-sample excluding statistical outliers, e.g. high-susceptibility samples. The latter must not be discarded automatically: they may isolate a subfabric of a different orientation or symmetry (i.e. L, S, etc.).
6. Geological information is required for a meaningful comparison of normalized versus non-normalized sample-tensors. The orientation-distributions alone do not suffice.
7. Non-orthorhombic symmetry of a sample-distribution indicates unsuitability for treatment as a tensor. The initial sample-size may have been too small to define the parent population-distribution, even if it was ideally orthorhombic and unimodal. Alternatively, the population-distribution may have been multi-modal. In either case, tensor statistics should not be abandoned: in the first instance, they provide the best estimate of the population, in the second they help identify fabric or mineralogical complexities.
8. When tensor-data are stacked from different subareas, the definition of the mean-tensor improves if the subareas are petrofabrically and structurally congruent.
9. The comparison of tensor-means for AMS and AARM in the same rocks provides a further interpretive tool, especially when normalized versus non-normalized data are compared.

Acknowledgements

This work was supported by operating and equipment grants to Graham Borradaile from NSERC (Ottawa, Canada). France Lacroix provided excellent research assistance while Sam Spivak and Anne Hammond provided invaluable technical support. I particularly thank Mike Jackson, as well as Frantisek Hrouda, Nigel Woodcock and Karel Schumann for correspondence and constructive reviews. The data used in this paper has been collected over the last decade using Sapphire Instruments equipment for AMS (SI2B induction coil unit). For AARM, an SI4 AF demagnetizer (peak field to 200 mT, DC bias field for ARM ~0.1 mT, applicable over any AF window) was

used in conjunction with a Czech AGICO JR5a automatic spinner magnetometer, or, in some instances, with an upgraded Molspin spinner magnetometer. I am grateful to all three manufacturers for service, upgrading and advice that went beyond the expected limits of commercial service.

References

- Borradaile, G.J., 1987. Anisotropy of magnetic susceptibility: rock composition versus strain. *Tectonophysics* 138, 327–329.
- Borradaile, G.J., 1988. Magnetic susceptibility, petrofabrics and strain. *Tectonophysics* 156, 1–20.
- Borradaile, G.J., 1991. Correlation of strain with anisotropy of magnetic susceptibility (AMS). *Pure Appl. Geophys.* 135, 15–29.
- Borradaile, G.J., Lacroix, F., 2001. Magnetic fabrics reveal Upper Mantle Flow fabrics in the Troodos Ophiolite Complex, Cyprus. *J. Struct. Geol.* in press.
- Borradaile, G.J., Mothersill, J.S., 1984. Coaxial deformed and magnetic fabrics without simply correlated magnitudes of principal values. *Phys. Earth Planet. Inter.* 35, 294–300.
- Borradaile, G.J., Dehls, J.F., 1993. Regional kinematics inferred from magnetic subfabrics in Archean rocks of Northern Ontario. *Can. J. Struct. Geol.* 15, 887–894.
- Borradaile, G.J., Kehlenbeck, M.M., 1996. Possible cryptotectonic magnetic fabrics in "Posttectonic" granitoid plutons of the Canadian Shield. *Earth Planet. Sci. Lett.* 137, 119–127.
- Borradaile, G.J., Henry, B., 1997. Tectonic applications of magnetic susceptibility and its anisotropy. *Earth Sci. Rev.* 42, 49–93.
- Borradaile, G.J., Puumala, M., Stupavsky, M., 1992. Anisotropy of complex magnetic susceptibility (ACMS) as an indicator of strain and petrofabric in rocks bearing sulphides. *Tectonophysics* 202, 309–318.
- Borradaile, G.J., Lacroix, F., King, D., 1998. Tilting and Transpression of an Archean Anorthosite in northern Ontario. *Tectonophysics* 293, 239–254.
- Borradaile, G.J., Fralick, P.W., Lacroix, F., 1999a. Acquisition of anhysteretic remanence and tensor subtraction from AMS isolates true palaeocurrent grain alignments. In: Tarling, D.H., Turner, P. (Eds.), *Palaeomagnetism and Diagenesis in Sediments*, pp. 139–145. Geological Soc. London, Spec. Publication 151.
- Borradaile, G.J., Werner, T., Lacroix, F., 1999b. Magnetic fabrics and anisotropy-controlled thrusting in the Kapuskasing Structural Zone, Canada. *Tectonophysics* 302, 241–256.
- Daly, L., Zinsser, H., 1973. Étude comparative des anisotropies de susceptibilité et d'aimantation rémanente isotherme: conséquences pour l'analyse structurale et le paléomagnétisme. *Ann. Géophys.* 29, 189–200.
- Dunlop, D.J., Özdemir, Ö., 1997. *Rock Magnetism: Fundamentals and Frontiers*. Cambridge Studies in Magnetism, Cambridge University Press, Cambridge, 573pp.
- Fisher, N.I., Lewis, T., Embleton, B.J.J., 1987. *Statistical Analysis of Spherical Data*. Cambridge University Press, Cambridge, 329pp.
- Flinn, D., 1965. On the symmetry principle and the deformation ellipsoid. *Geol. Mag.* 102, 36–45.
- Fuller, M.D., 1963. Magnetic anisotropy and paleomagnetism. *J. Geophys. Res.* 68, 293–309.
- Henry, B., 1989. Magnetic fabric and orientation tensor of minerals in rocks. *Tectonophysics* 165, 21–27.
- Hrouda, F., 1982. Magnetic anisotropy of rocks and its application in geology and geophysics. *Geophys. Surv.* 5, 37–82.
- Hrouda, F., Schulmann, K., 1990. Conversion of the magnetic susceptibility tensor into the orientation tensor in some rocks. *Phys. Earth and Planet. Interiors* 63, 71–77.
- Hrouda, F., Jelinek, J., 1999. Theoretical models for the relationship between magnetic anisotropy and strain: effect of triaxial magnetic grains. *Tectonophysics* 301, 183–190.

- Hrouda, F., Henry, B., Borradaile, G.J., 2000. Limitations of tensor subtraction in isolating diamagnetic fabrics by magnetic anisotropy. *Tectonophysics* 322, 303–310.
- Jackson, M., 1991. Anisotropy of magnetic remanence: a brief review of mineralogical sources, physical origins, and geological applications and comparison with susceptibility anisotropy. *Pure Appl. Geophys.* 136, 1–28.
- Jelinek, V., 1978. Statistical processing of anisotropy of magnetic susceptibility measured on groups of specimens. *Studia geoph. et geodetica.* 22, 50–62.
- Jelinek, V., 1981. Characterization of the magnetic fabric of rocks. *Tectonophysics* 79, 63–67.
- Jelinek, V., 1993. Theory and measurement of the anisotropy of isothermal remanent magnetization of rocks. *Travaux Géophysiques* 37, 124–134.
- Lagroix, F., Borradaile, G.J., 2000. Tectonics of the circum-Troodos sedimentary cover of Cyprus, from rock magnetic and structural observations. *J. Struct. Geol.* 22, 453–469.
- Lienert, B.R., 1991. Monte Carlo simulation of errors in the anisotropy of magnetic susceptibility: a second rank symmetric tensor. *J. Geophys. Res.* 96, 19539–19544.
- Lisle, R.J., 1989. The statistical analysis of orthogonal orientation data. *J. Geol.* 97, 360–364.
- Nakamura, N., Borradaile, G.J., 2001. Strain, anisotropy of anhysteretic remanence, and anisotropy of magnetic susceptibility in a slaty tuff. *J. Struct. Geol.* under review.
- Nye, J.F., 1957. *Physical Properties of Crystals*. Oxford University Press, New York, 329pp.
- Ramsay, J.G., 1967. *Folding and Fracturing of Rocks*. McGraw-Hill, New York, 568pp.
- Rochette, P., Jackson, M.J., Aubourg, C., 1992. Rock magnetism and the interpretation of anisotropy of magnetic susceptibility. *Rev. Geophys.* 30, 209–226.
- Scheidegger, A.E., 1965. On the statistics of the orientation of bedding planes, grain axes, and similar sedimentological data. *US Geol. Survey, Prof. Paper* 525-C, 164–167.
- Stephenson, A., Sadikun, S., Potter, D.K., 1986. A theoretical and experimental comparison of the anisotropies of magnetic susceptibility and remanence in rocks and minerals. *Geophys. J. R. Astr. Soc.* 84, 185–200.
- Uyeda, S., Fuller, M.D., Belshe, J.C., Girdler, R.W., 1963. Anisotropy of magnetic susceptibility of rocks and minerals. *J. Geophys. Res.* 68, 279–291.
- Woodcock, N.H., 1977. Specification of fabric shapes using an Eigenvalue method. *Geol. Soc. Am. Bull.* 88, 1231–1236.